

1 **Global Atmospheric Carbon Budget: results from an**
2 **ensemble of atmospheric CO₂ inversions**

3
4 **P. Peylin¹, R. M. Law², K. R. Gurney³, F. Chevallier¹, A. R. Jacobson⁴, T.**
5 **Maki⁵, Y. Niwa⁵, P. K. Patra⁶, W. Peters⁷, P. J. Rayner^{1,8}, C. Rödenbeck⁹, X.**
6 **Zhang³**

7 [1]{Laboratoire des Sciences du Climat et de l'Environnement, Gif sur Yvette, France}

8 [2]{Centre for Australian Weather and Climate Research, CSIRO Marine and
9 Atmospheric Research, Aspendale, Australia}

10 [3]{School of Life Sciences/Global Institute of Sustainability, Arizona State University,
11 Tempe, USA}

12 [4]{University of Colorado and NOAA Earth System Research Laboratory, Boulder,
13 USA}

14 [5]{Meteorological Research Institute, Tsukuba, Japan}

15 [6]{Research Institute for Global Change, JAMSTEC, Yokohama, Japan}

16 [7]{Dept. of Meteorology and Air Quality, Wageningen University, Wageningen,
17 Netherlands}

18 [8]{School of Earth Sciences, University of Melbourne, Parkville, Australia}

19 [9]{Max-Planck-Institute for Biogeochemistry, Jena, Germany}

20 Correspondence to: P. Peylin (peylin@lsce.ipsl.fr)

21
22 **Supplementary material**

23 **Description of inversions**

24 A short description of the different inversions is provided below, and a list of stations for
25 each inversion can be found in the section “Observational constraints used by the
26 participating inversion systems”, or under: <https://transcom.lsce.ipsl.fr>.

27 **LSCE_analytical (LSCEa):**

28 LSCEa corresponds to the results described in Piao et al., 2009, the sensitivity test
29 without Siberian vertical profiles. It is based on a “matrix” formulation (see Peylin et al.,
30 2005). **Fluxes:** solved at the spatial resolution of the transport model and monthly
31 resolution; prior land fluxes taken as the climatology over 1996-2004 from the
32 ORCHIDEE model (Krinner et al., 2005); prior ocean fluxes from Takahashi et al.,
33 (2002). Prior land/ocean errors set to 6.0/2.5 Pg C yr⁻¹ globally and spatially distributed
34 according to the Gross Primary Production of ORCHIDEE / the surface area of ocean
35 grid cells; flux error correlations between land/ocean grid-points, following an e-folding
36 length of 1000/2000 km. **Observations:** 73 sites from GLOBALVIEW-CO₂ and
37 CARBOEUROPE EU-project (9 sites); Errors (measurements + model) range between
38 0.4 ppm for remote stations (South Pole) and 3 ppm for continental sites (Hungaria).
39 **Prescribed fluxes:** fossil fuel with spatial distribution from Oliver and Berdowski (2001)
40 and annual totals rescaled each year for each country using CDIAC statistics; Biomass
41 burning from van der Werf et al. (2006).

42 **LSCE_variational (LSCEv):**

43 LSCEv corresponds to the results described in Chevallier et al., 2010,. It is based on a
44 variational formulation (see Chevallier et al., 2005), with posterior errors provided by a
45 robust Monte Carlo approach. Fluxes: solved at the spatial resolution of the transport
46 model and at weekly resolution; prior land fluxes from the ORCHIDEE model at
47 appropriate date for natural vegetation (Krinner et al. 2005), from the fossil fuel
48 inventory of Oliver and Berdowski (2001) with annual global totals rescaled using
49 CDIAC statistics, from the biomass burning estimates of Randerson et al. (2007); prior
50 ocean fluxes from Takahashi et al., (2009). Prior land/ocean errors set to 3.6/0.9 PgC y⁻¹
51 globally and spatially distributed according to the heterotrophic respiration of
52 ORCHIDEE / the surface area of ocean grid cells; flux error correlations between
53 land/ocean grid-points, following an e-folding length of 500/1000 km. Observations: 128

54 sites from a series of global databases; Errors (measurements + model) range between a
55 few tenths of a ppm for marine stations and up to 6 ppm for continental sites (CBW).

56 **CTracker US (CT2009):**

57 CarbonTracker is an ongoing program of the United States National Oceanic and
58 Atmospheric Administration (NOAA) to publish approximately-annual estimates of CO₂
59 surface exchange over the globe. The 2009 update of CarbonTracker (CT2009) used here
60 is a revised version of the system described in Peters et al. (2007) and is fully
61 documented online at <http://www.esrl.noaa.gov/gmd/ccgg/carbontracker/CT2009/>.

62 CarbonTracker uses an ensemble Kalman filter scheme to estimate weekly scaling factors
63 multiplying prior-model net carbon exchange over 126 land and 30 ocean regions
64 covering the globe. Flask and quasi-continuous observations from 94 sites of the CO₂
65 observing networks operated by NOAA, Environment Canada, the Australian
66 Commonwealth Scientific and Industrial Research Organization (CSIRO), the National
67 Center for Atmospheric Research (NCAR), and Lawrence Berkeley National Laboratory
68 are assimilated to produce optimal surface flux estimates. A relatively short assimilation
69 window of five weeks is used to determine adjustments to surface fluxes. Model-data
70 mismatch errors assigned to observations range from 0.75 to 7.5 ppm. Atmospheric
71 transport is simulated with the nested-grid TM5 model described in Krol *et al.* (2005),
72 using winds from the operational forecast model of the European Centre for Medium-
73 Range Weather Forecasts.

74 CarbonTracker simulates four types of CO₂ exchange with the atmosphere. Fossil-fuel
75 and biomass burning estimates are imposed without modification, and air-sea exchange
76 and non-wildfire land exchange are subject to optimization.

77 Annual country-total fossil fuel emissions for CT2009 were derived from Carbon
78 Dioxide Information and Analysis Center (CDIAC) estimates of Andres *et al.* 2009
79 through 2006, then extrapolated for 2007 and 2008, using relative increases for each fuel
80 type from the BP Statistical Review of World Energy. These emissions are distributed
81 spatially according to EDGAR v4 inventory estimates, and an annual cycle is applied
82 between 30°N and 60°N, as detailed in the online documentation for CT2009. Land
83 biosphere priors are supplied by the Global Fire Emissions Database (GFED) version 2 of

84 van der Werf *et al.* (2006). Air-sea exchange of CO₂ is derived from the ocean interior
85 inversions of Jacobson *et al.* (2007), and includes a trend in anthropogenic CO₂ uptake by
86 the world ocean.

87 Compared to the CT2007 release described in Peters et al (2007), the following
88 significant changes have been made in CT2009: i) Observations from 12 new quasi-
89 continuous stations have been used as assimilation constraints; ii) Seasonality of fossil
90 fuel emissions has been extended to the entire Northern Hemisphere north of 30°N; iii)
91 The air-sea CO₂ flux prior is now time-varying and comes from the ocean inversions
92 reported in Jacobson *et al.* (2007). The number of ocean regions has been increased to 30
93 from its original 11. The resolution of atmospheric transport in the global domain has
94 been increased to 3°x2° (N. American transport remains at 1°x1°).

95 **CTracker Europe (CTE2008):**

96 CarbonTracker Europe is based on the exact same inversion framework as
97 CarbonTracker US described above. It differs in a number of important choices for the
98 inputs, specifically:

- 99 • CT Europe uses a set of 23 CarboEurope CO₂ mole fraction observations not
100 available in CT US,
- 101 • CT US uses CSIRO CO₂ mole fraction observations which were not assimilated
102 in CT Europe,
- 103 • CT Europe uses a TM5 two-way nested transport grid with highest 1x1 degree
104 resolution over Europe instead of over North America,
- 105 • CT Europe uses a different seasonality of European fossil fuel emissions (based
106 on work from the Institut für Energiewirtschaft und Rationelle Energieanwendung
107 (IER), Stuttgart),
- 108 • CT Europe has an increased number of European vegetation types (38 instead of
109 19 possible types) for which weekly parameters are optimized.

110 **CCAM and MATCH:**

111 The CCAM and MATCH inversions use a Bayesian synthesis method and are described
112 in Rayner et al. (2008), except that the time period of the inversions has been extended to
113 2008 and a slightly different set of observing sites has been used. The CCAM and
114 MATCH inversions set up is identical except for the transport model used (CCAM or
115 MATCH) and the number of regions solved for (CCAM: 94 land, 52 ocean, MATCH: 67
116 land, 49 ocean). Neither transport model used interannual-varying winds. **Fluxes:** Land
117 fluxes are solved relative to a CASA climatology (Randerson et al., 1997). Most land
118 priors are zero relative to CASA with some non-zero priors representing land-use change.
119 Ocean fluxes are solved relative to the climatology of Takahashi et al. (1999) with prior
120 fluxes of zero. Prior land uncertainties are scaled by NPP while ocean uncertainties are
121 scaled by region area with total uncertainty similar to Baker et al. (2006). **Prescribed**
122 **fluxes:** fossil emissions follow a spatial distribution which is a linear combination of
123 Andres et al. (1996) representing 1990 and Brenkert (1998) representing 1995, scaled to
124 annual totals from CDIAC. **Observations:** 73 CO₂ records from GLOBALVIEW-CO2
125 (2009), used as monthly means, 7 $\delta^{13}\text{CO}_2$ records from CSIRO (Francey et al., 1996).
126 Data uncertainties range from 0.3-9.2 ppm and vary in time. Larger uncertainties are used
127 for periods with extrapolated data from GLOBALVIEW.

128 **JENA s96-v3.3 (JENA):**

129 **Observations:** Data from 52 sites whose records span the whole inversion period (1996-
130 2009). Flask pair values or hourly values, respectively, are used directly at their time of
131 measurement. Hourly data are selected for daytime or nighttime values at certain sites
132 (see Table at the end of the Supplementary material). **Fluxes:** Estimated at the spatial
133 resolution of the transport model and daily time steps, with a-priori spatial and temporal
134 correlations (decaying with distance). Prior fluxes are constant in time, in order not to
135 influence variability of the estimates. **Prescribed fluxes:** Fossil fuel emissions from
136 EDGAR 4.0 (linearly extrapolated after 2005 using BP global totals). **Solution method:**
137 Conjugate Gradients minimization with re-orthonormalization after each iteration.

138 Jena inversion runs are also available for longer time periods (starting 1981 using 15
139 long-record sites), or using more sites (up to 61, for shorter periods over which all sites

140 provide data). All results, including regular updates, can be downloaded from
141 “<http://www.bgc-jena.mpg.de/~christian.roedenbeck/download-CO2/>”.

142 **TRANSCOM_mean (TrC):**

143 The TransCom mean results are based on the TransCom 3 Level 2 analysis found in
144 Gurney et al. (2008) and Baker et al., 2006, but the observational time series have been
145 extended to 2008 (inclusive). The individual posterior flux results (from 11 transport
146 models) are averaged to generate the multi-model mean. The observational time series
147 spans the 1990 to 2008 time period with a total of 103 observing sites from the
148 GLOBALVIEW-CO₂ database. The inversion approach used in the TransCom 3 Level 2
149 results follows the Bayesian synthesis method (Enting 2002). There are 11 land and 11
150 ocean basis functions that are roughly sub-continental in size. The four background
151 carbon fluxes consisted of 1990 and 1995 fossil fuel emission fields (Andres et al., 1996;
152 Brenkert, 1998), an annually-balanced, seasonal biosphere exchange (Randerson et al.,
153 1997), and air-sea gas exchange (Takahashi et al., 1999). These fluxes are included in the
154 inversion with a small prior uncertainty so that their magnitude is effectively fixed.

155 **RIGC TDI-64 (RIGC):**

156 This Bayesian time-dependent inversion with 64-regions (**TDI-64**) is developed based on
157 the TransCom level 3 inverse model in order to increase the degrees of freedom for flux
158 estimation (or reduce regional aggregation error). The 11 land and 11 ocean regions are
159 divided into 42 and 22 regions, respectively (detailed sensitivity tests for prior flux and
160 data uncertainties/network are discussed in Patra et al., 2005). By this division, we are
161 able to draw distinction between the east and west or north and south of 10 TransCom
162 land regions, and north and south of the Tropical Asia and all ocean regions.
163 **Atmospheric CO₂** time series from 74 GLOBALVIEW-CO₂ sites are used with their
164 corresponding uncertainty derived from climatology of the monthly mean residuals plus
165 0.3 ppm as a measure of the model representation error. The data uncertainty varies from
166 0.31 ppm at SPO to 4.6 ppm at HUN and 5.1 ppm at BSC. The NIES/FRCGC **transport**
167 **model** (Maksyutov et al., 2008) is driven by interannually varying NCEP reanalysis
168 meteorology. The **pre-subtracted fluxes** are taken from CASA terrestrial ecosystem
169 model (Randerson et al., 1997) and Takahashi et al. (2009) climatology for oceanic

170 exchange at monthly time intervals. Fossil fuel emission distributions are taken from
171 EDGAR4.0 and global totals are scaled to CDIAC estimated annual emissions. Prior flux
172 uncertainties are assigned in range of $\sim 0.37 \text{ PgCy}^{-1}$ to $\sim 2.12 \text{ PgCy}^{-1}$ for both land and
173 ocean regions.

174 **JMA 2010 (JMA):**

175 JMA inversion method corresponds to the method described in Maki et al. 2010 which is
176 based upon Transcom 3 IAV inversion set up (Baker et al. 2006) with real observation
177 data (WDCGG) and interannual varying wind (JRA25). The analysis period is extended
178 and some modifications are done. **Fluxes:** solved at the spatial resolution of 22 regions
179 and monthly resolution; prior land fluxes taken as the climatology from CASA model;
180 prior ocean fluxes from Takahashi et al., (2002). Prior land/ocean errors set to Transcom
181 3 IAV uncertainties; flux error correlations are set to zero. **Observations:** 146 sites from
182 WDCGG monthly mean CO_2 concentrations after site selection by mismatch between
183 observation and inversion; Errors (measurements + model) range between 0.3 ppm for
184 remote stations (South Pole) and 5 ppm for continental sites. **Prescribed fluxes:** fossil
185 fuel with spatial distribution from Andres et al. (1996) and Brenkert (1998) annual totals
186 rescaled each year for each country using CDIAC statistics.

187 **NICAM-TM (NICAM):**

188 NICAM-TM inversion system is described by Niwa et al. (2012). While Niwa et al.
189 (2012) extensively used aircraft measurements from CONTRAIL this inversion used only
190 surface measurements and limited aircraft measurements. The inversion method and
191 setup are similar to those of TRANSCOM. **Fluxes:** the spatial number of fluxes solved
192 by the inversion is 29 and 11 respectively for land and ocean. The 29 land regions were
193 obtained by dividing the 11 regions of TRANSCOM (slightly different from 31 regions
194 of Niwa et al. (2012)). The ocean flux partitioning is the same as TRANSCOM. The prior
195 land flux is taken from the climatology flux of CASA (Randerson et al. 1997); the prior
196 ocean flux is from Takahashi et al., (2009). Prior land flux errors are given by
197 redistributing those for the 11 regions of TRANSCOM into the 29 regions according to
198 NPP distributions, whereas prior ocean flux errors are the same as those of TRANSCOM.
199 There is no error correlation for the prior fluxes. **Observations:** 94 sites from

200 GLOBALVIEW-CO₂ and 9 sites from Siberian aircraft data of NIES; Errors
201 (measurements + model) range between 0.3 ppm for remote stations and 6.6 ppm for
202 continental sites (LEF) (monthly mean). *Prescribed fluxes*: fossil fuel with spatial
203 distribution from EDGAR version 4.1 and annual totals rescaled each year for each
204 country using CDIAC statistics.
205

206 **Additional figures**

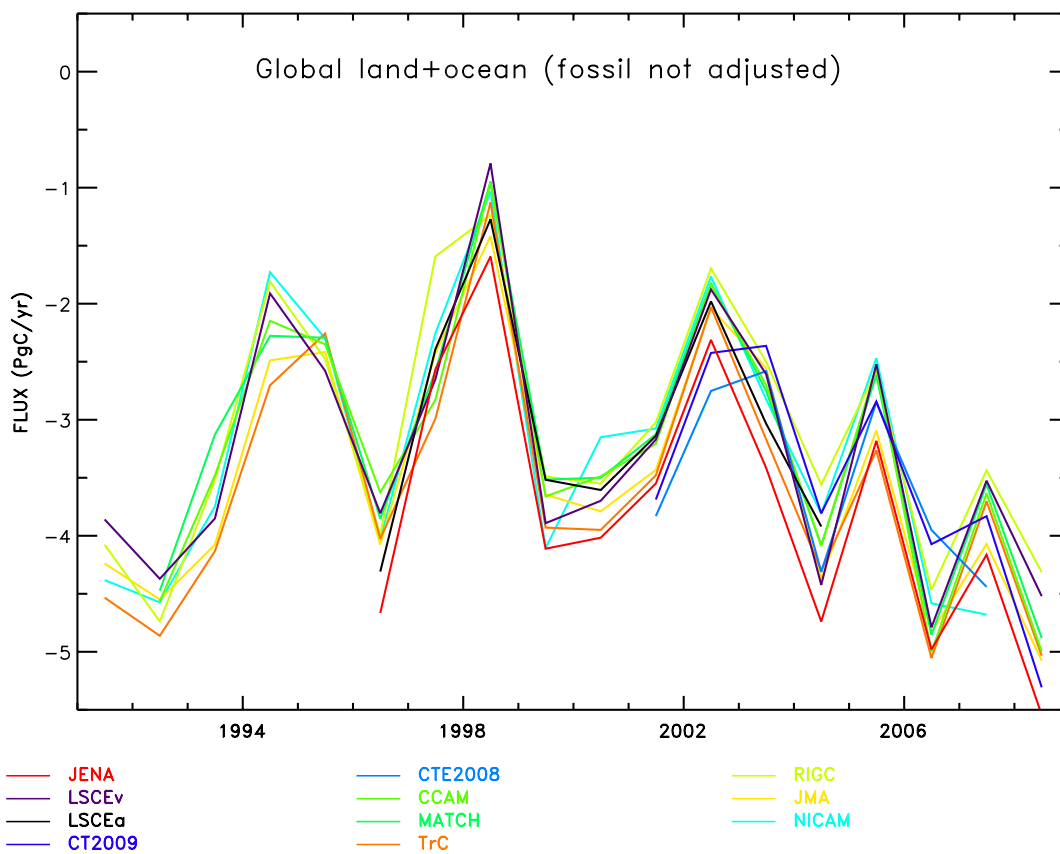
207 This appendix provides additional figures showing the estimated and prior aggregated
208 carbon fluxes (Figures S1 to S6) as well as the region boundaries used to aggregate the
209 fluxes (Figure S7) and the spatial flux distribution (Figure S8).

210

211

212

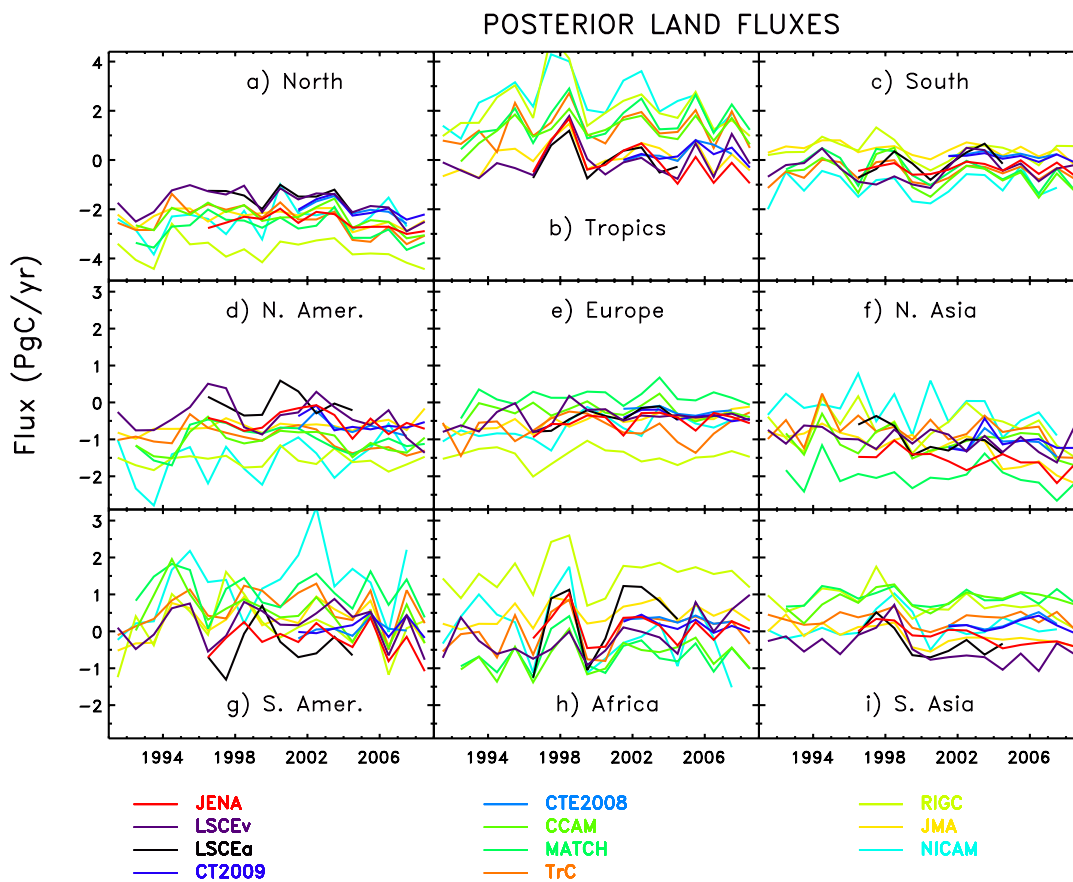
213



214

215 Figure S1: Annual mean posterior flux of the individual participating inversions for
216 natural global total carbon exchange without fossil correction.

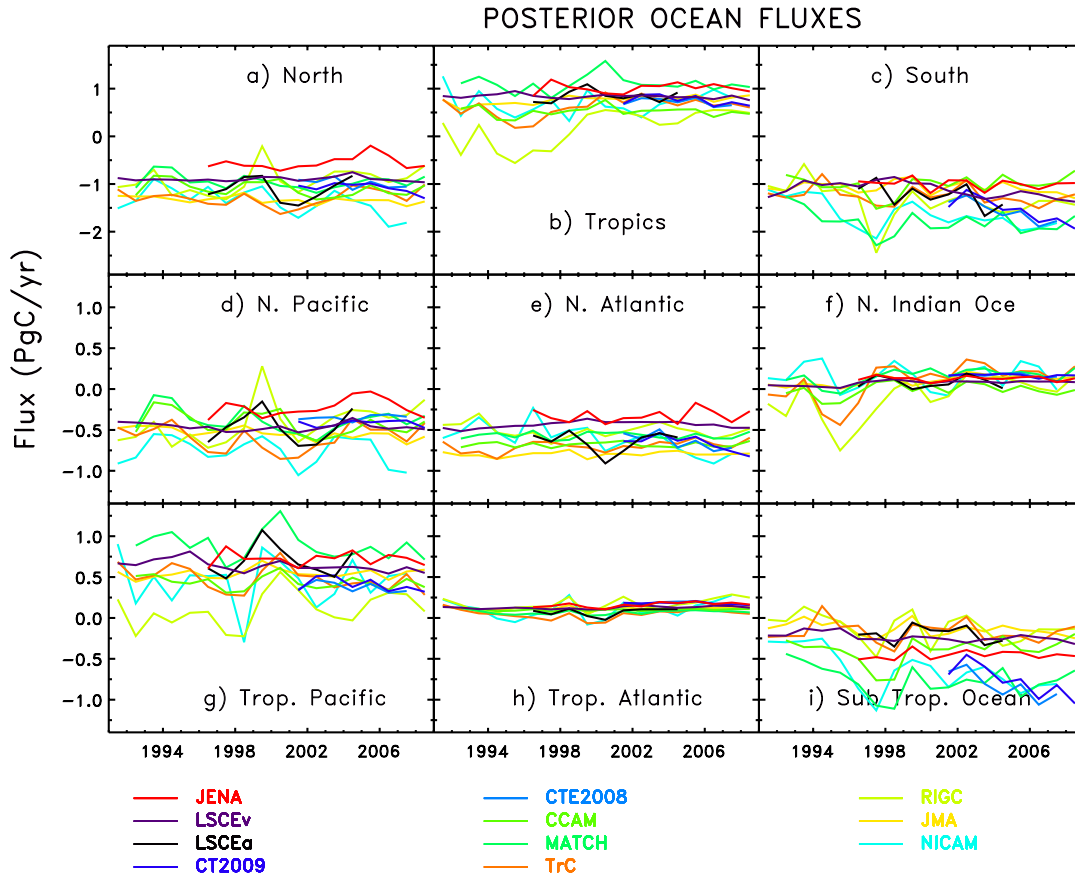
217



218

219 Figure S2: Annual mean posterior natural land flux estimate of the individual
 220 participating inversions. Shown here are a) North ($>25^{\circ}\text{N}$) b) Tropics ($25^{\circ}\text{S} << 25^{\circ}\text{N}$), c)
 221 South ($<25^{\circ}\text{S}$) d) North America, e) Europe, f) North Asia, g) South America, h) Africa, i)
 222 South Asia.

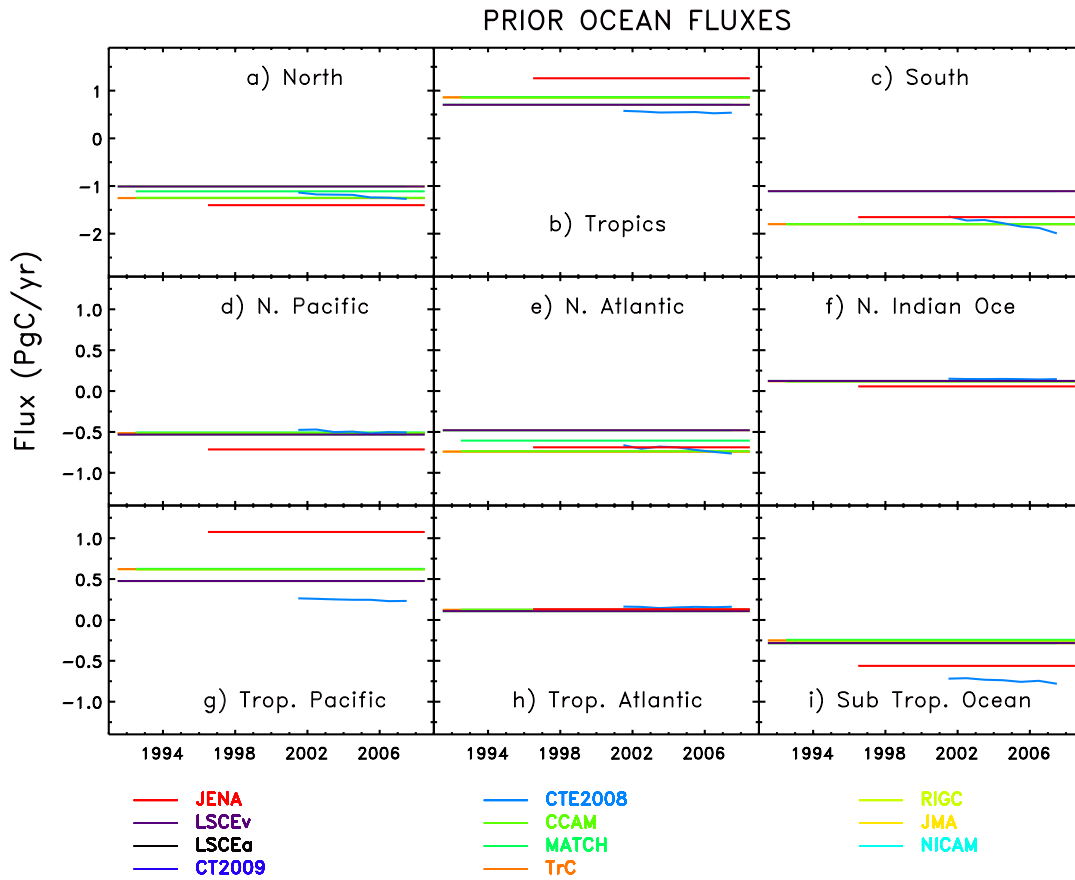
223



227

228 Figure S4: Annual mean posterior natural ocean flux estimate of the individual
 229 participating inversion. Shown here are a) North (>25N) b) Tropics (25S<<25N), c)
 230 South (<25S) d) North Pacific, e) North Atlantic, f) Tropical Indian ocean, g) Tropical
 231 Pacific, h) Tropical Atlantic, i) Sub tropical ocean.

232



233

234 Figure S5: Same as Fig. S4 but for the Prior ocean fluxes.

235

236

237

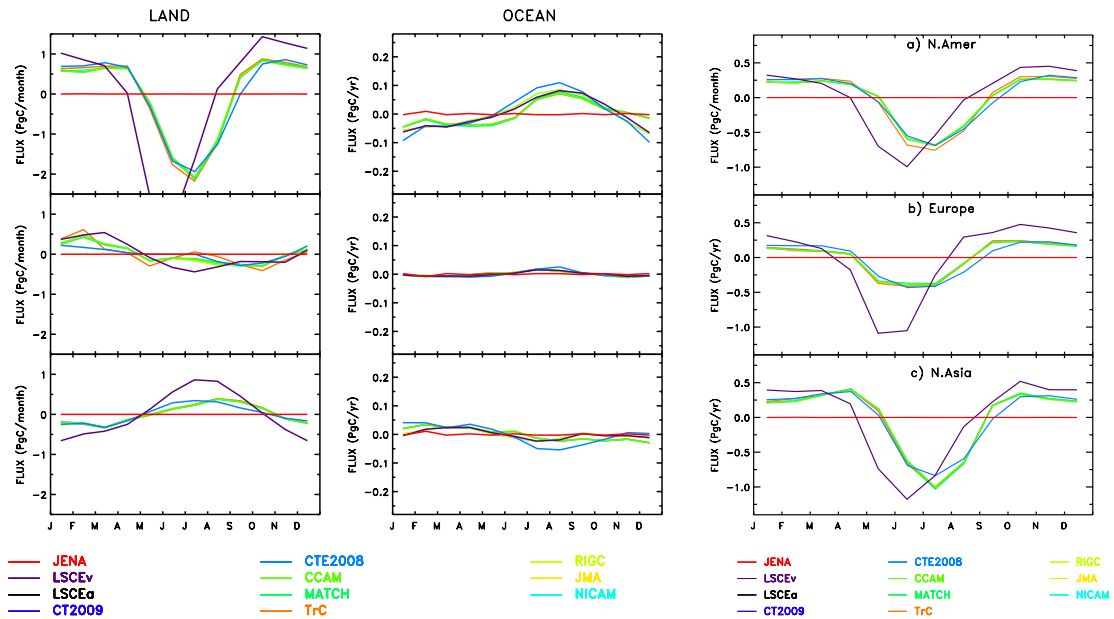


Figure S6: Mean seasonal cycle for the prior fluxes from most participating models for selected regions

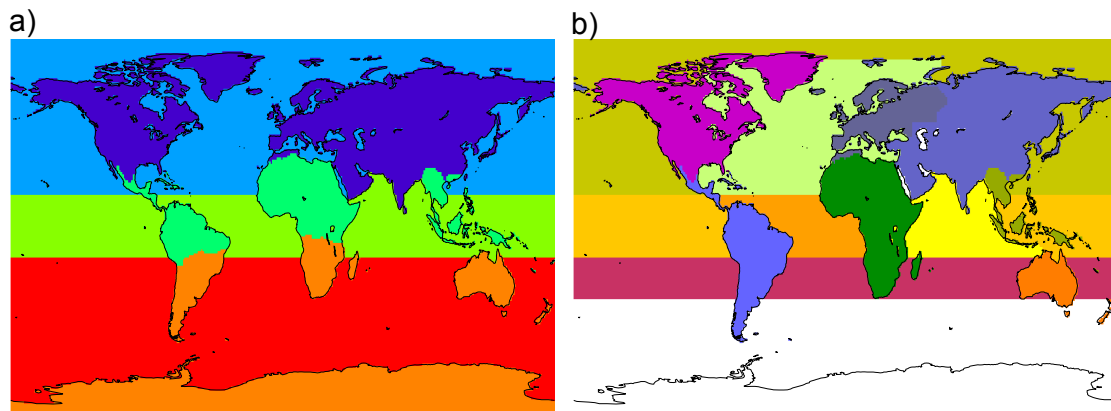


Figure S7: Region boundaries used for the aggregated fluxes: a) latitudinal breakdown (north, tropics, south) for land and ocean; b) continental breakdown used for north America, Europe, north Asia, south America, Africa, tropical Asia, Australia, north Pacific, north Atlantic, tropical Pacific, tropical Atlantic, Indian Ocean, sub-tropical Ocean.

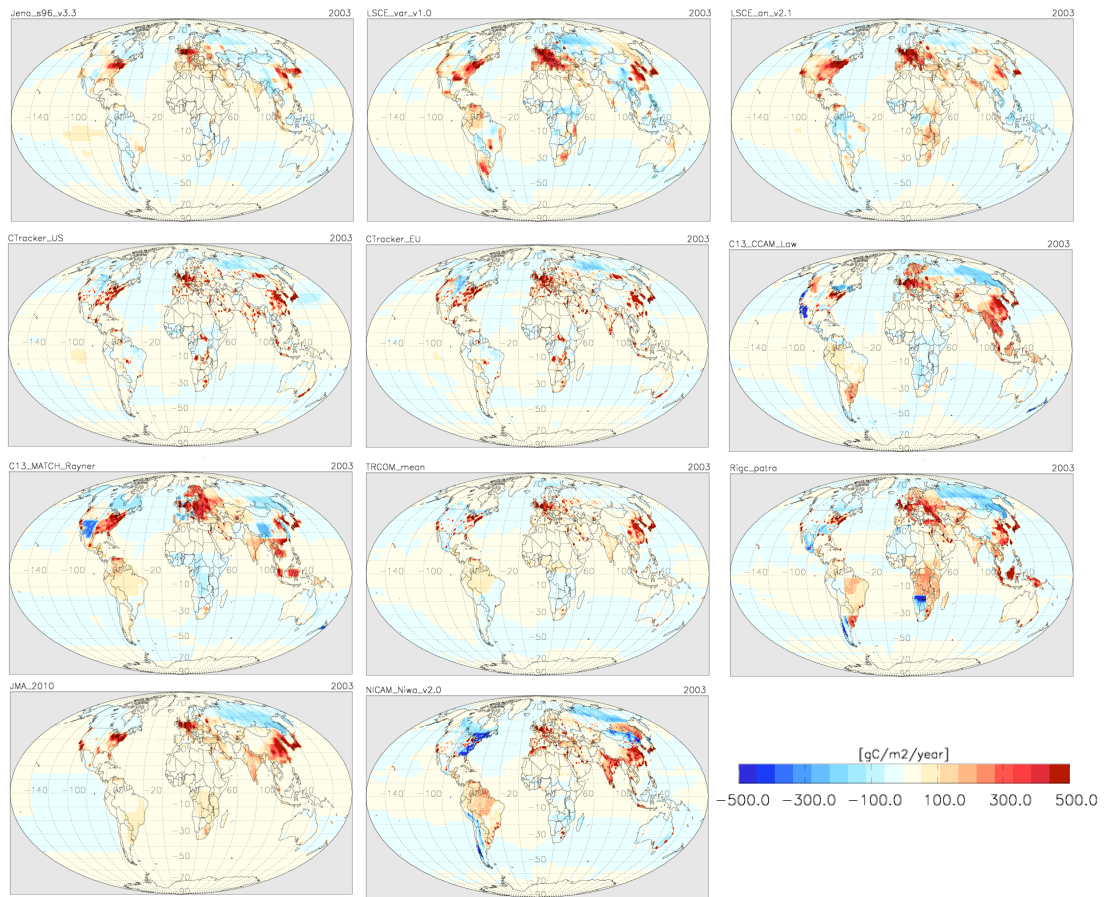


Figure S8: Spatial distribution of the annual natural fluxes (without fossil correction) for 2003 for the participating inversions.

Observational constraints used by the participating inversion systems

Sites are listed alphabetically, in general using the site codes of GLOBALVIEW (www.esrl.noaa.gov/gmd/ccgg/globalview/co2/co2_observations.html). Many site locations are listed more than once, since multiple CO₂ records are available for many sites (either collected by different labs, or representing separate flask and in-situ records). Some inversions chose only to use the most complete record at a given location while others include all available records. It is unlikely that one choice is better than the other. There are differences in calibration etc between laboratories. These are not accounted for in inversions, but their impact is unlikely to be significant compared to other transport and representation uncertainties in modelling any given site (Rödenbeck et al., 2006).

Type of observed CO₂ used for each site: There are a variety of ways the CO₂ data from any given site has been used, depending in part on whether flask or in-situ data are available; some inversions use monthly mean data while others use the data at the appropriate sampling time. Various degrees of selection have been applied to the data. An indication of how the data have been used is given in the table through a series of codes.

Code	Explanation
<i>Temporal resolution</i>	
M	Monthly mean data used
D	Daily mean data used
H4	Four hour mean data used
H4 (hrs)	Four hour mean data used only for the hours indicated (UT)
H	Hourly data used
H (hrs)	Hourly data used only for the hours indicated (UT)
F4	Flask samples are used as a 4 hour average around sampling time
F	Flasks samples are used at the sampling time
<i>Data selection</i>	
GV	Globalview CO ₂ used. Globalview CO ₂ is derived from a fitted curve to CO ₂ observations

	and is intended to represent baseline conditions
GV E	The use of Globalview CO ₂ data includes extrapolated data. This fills in missing data by applying a mean seasonal offset for the site from marine boundary layer CO ₂ concentration. Many inversions give periods of extrapolated data less weight than periods with observations.
*	Consecutive hours that differ by greater than 1 ppm are removed
o	Outliers (mismatch between observations and model > 3 sigma) are removed
JMA	Data are removed when inconsistent with the inversion through an iterative procedure (Maki et al., 2010)

Site locations may be represented by model output interpolated to the site location or by the nearest model grid-cell. For coastal sites, the nearest ocean grid-cell is often chosen as being more representative of the baseline air that is usually sampled by flask records at coastal sites.

Some inversions include ship data. This may be used at the actual location and time of sampling (as in the CarbonTracker inversions) or it may be binned into latitude and/or longitude bins as in the GLOBALVIEW POC* records and the JMA use of JMA ship data.